Kidney International, Vol. 58 (2000), pp. 618–628

Interstitial fibrosis in mice with overload proteinuria: Deficiency of TIMP-1 is not protective

Allison A. Eddy, Heungsoo Kim, Jesús López-Guisa, Takashi Oda, and Paul D. Soloway, with the technical assistance of Lori McCulloch, Elaine Liu, and Diane Wing

The Children's Hospital and Regional Medical Center, University of Washington, Seattle, Washington, and Department of Molecular and Cellular Biology, Roswell Park Cancer Institute, Buffalo, New York, USA; and the Hospital for Sick Children, Department of Pediatrics, University of Toronto, Toronto, Canada

Interstitial fibrosis in mice with overload proteinuria: Deficiency of TIMP-1 is not protective.

Background. Progressive renal interstitial fibrosis is characterized by up-regulated expression of the gene that encodes the tissue inhibitor of metalloproteinases-1 (TIMP-1), a regulator of extracellular matrix remodeling, suggesting that impaired matrix turnover contributes to the fibrogenic process. The present study was designed to develop a murine model of renal interstitial fibrosis, and to determine the functional significance of up-regulated *Timp-1* expression by comparing the severity of this renal disease in wild-type mice and mice genetically deficient in *Timp-1*.

Methods. Initial pilot studies developed and characterized a murine model of bovine serum albumin (BSA)-induced protein-overload proteinuria with respect to the degree of proteinuria, severity of interstitial fibrosis, and renal mRNA levels for genes encoding matrix proteins, transforming growth factor-β1 (TGF-β1), and TIMP-1, -2, -3, and -4. In the final study, the severity of interstitial fibrosis was compared in wild-type and *Timp-1*–deficient mice after six weeks of proteinuria.

Results. Mice injected with large daily intraperitoneal doses of BSA developed proteinuria, interstitial inflammation, and progressive interstitial fibrosis. A time course study based on measurements after one, two, and six weeks of BSA injections showed increased renal mRNA levels for the matrix genes procollagens α1(I), α1(III), and α2(IV) and TGF-β1 and *Timp-1*. *Timp-2* and *Timp-3* genes were constitutively expressed at high levels in the normal kidneys and showed little change in the proteinuric kidneys. *Timp-4* transcripts were not detected in any of the kidneys. After six weeks of BSA overload-proteinuria, the groups ($N = 8$ per group) of wild-type and *Timp-1*–deficient mice developed significant interstitial fibrosis compared with the control saline-injected groups. The severity of the interstitial fibrosis was similar in both proteinuric groups based on an assessment of the final kidney weight, total kidney collagen content, and the number of interstitial fields with increased fibronectin staining.

Conclusions. Results of the present study indicate that TIMP-1 deficiency does not alter the degree of interstitial fibrosis in the murine overload proteinuria model. Potential explanations include *Timp-1* genetic redundancy, as suggested by the observation that, despite significant intrarenal induction of the *Timp-1* gene expression, net renal metalloproteinase-9 (MMP-9) activity was not significantly altered. TIMP-1 is a multifunctional protein that may play a metalloproteinase-independent role in response to renal injury.

Key words: tissue inhibitor of metalloproteinase, fibrosis, murine model, renoprotection, proteinuria.

Received for publication October 29, 1999
and in revised form February 18, 2000
Accepted for publication March 12, 2000

Progressive renal disease is characterized histologically by interstitial fibrosis, tubular atrophy, and the disappearance of peritubular capillaries. The process of interstitial fibrogenesis is currently considered to be the primary final common pathway that leads to progressive renal insufficiency [1]. The specific molecular pathways that initiate fibrosis are currently under intensive investigation. Within the tubulointerstitial compartment of the kidney, transforming growth factor-β1 (TGF-β1), connective tissue growth factor, endothelin-1, and angiotensin II appear to play important initiating roles. These fibrogenic molecules activate several genetic programs that cause scarring caused by both increased rates of matrix protein synthesis and perturbations in matrix remodeling and turnover. The relative importance of the synthesis and turnover pathways is currently unknown.

Although it seems clear that increased rates of matrix protein synthesis make an important contribution to renal interstitial fibrosis, there is increasing evidence that impaired degradation of interstitial matrix proteins also plays a significant role. The importance of the latter pathway was first highlighted by the studies of González-Avila, Vadillo-Ortega, and Pérez-Tamayo [2]. They ligated the renal vein or one ureter of rats to cause severe renal fibrosis. Their studies did not find increased collagen synthesis rates; they documented impressive 30-fold and 10-fold reduc-

tions, respectively, in renal collagenolytic activity. Normal kidneys produce a number of proteases that have specificity for matrix proteins, including several enzymes that belong to the metalloproteinase family [3, 4]. Several studies on the pathogenesis of renal interstitial fibrosis have found no significant differences in renal mRNA levels for the metalloproteinases [5, 6]. In contrast, significantly increased expression of the inducible inhibitor tissue inhibitor of metalloproteinases-1 (in this article, the following abbreviations are used for the tissue inhibitor of metalloproteinases: TIMP-1, the protein; *Timp-1*, murine normal gene or mRNA; and *timp*-1, mutant murine allele) has been reported in most of the experimental models of chronic renal disease that have been investigated. For example, *Timp-1* mRNA levels are increased in association with interstitial fibrosis in antitubular basement membrane nephritis [7], cyclosporine nephropathy [8], diabetic nephropathy [9], hypercholesterolemia [10], murine lupus nephritis [11], obstructive uropathy [12–14], polycystic kidney disease [15], protein overload proteinuria [6], and puromycin aminonucleoside nephrosis [5, 16]. Available data from in situ hybridization studies suggest that both tubular epithelial cells and interstitial cells produce TIMP-1 in the renal tubulointerstitium [17].

The goal of the present study was to determine the functional significance of TIMP-1 overexpression by comparing the severity of interstitial fibrosis in mice genetically deficient in TIMP-1 to renal disease severity in wild-type mice from the same genetic background. To perform these studies, it was first necessary to develop a reliable murine model of renal interstitial fibrosis. Despite the availability of several potentially interesting transgenic mice, renal research has been hampered by the lack of appropriate murine renal disease models. The best characterized mouse models are genetic renal diseases such as murine lupus nephritis and polycystic kidney disease. Studies based on these genetic models introduce the need for complex cross-breeding strategies in order to use the genetic manipulations that have been introduced into transgenic mice. Immunologic models of renal disease show tremendous strain-dependent disease susceptibility. For example, the C57BL/6 strain that is commonly used to generate transgenic mice is resistant to autoimmune antitubular basement membrane disease [18]. Drugs such as the aminonucleoside of puromycin do not have nephrotoxic effects in mice. The model of unilateral ureteral obstruction is associated with severe interstitial fibrosis [19], but the relevance of this model to human disease is unclear, as postnatal ureteral obstruction in humans does not have such short-term devastating effects. Based on our previous experience with the rat model of bovine serum albumin (BSA)-induced overload proteinuria, the present study reports the reproducibility of this model in mice. One previous study reported the presence of transient proteinuria in mice after a single intraperitoneal injection of a large dose of BSA, but chronic studies have not been reported previously [20].

METHODS

Murine protein-overload proteinuria: Development of the model

B6SJL mice weighing approximately 20 g were purchased from the Jackson Laboratory (Bar Harbor, ME, USA). TIMP-1–deficient mice and wild-type controls on the $129Sv^{Jae}$ background are described elsewhere [21]. Since the *Timp-1* gene is located on the X chromosome [22], we chose to perform all studies in male mice. The genotype of each male was determined by polymerase chain reaction analyses of tail vein DNA using four primer sequences that amplified the neomycin gene insert in the mutant mice to give a 477 nucleotide product and a 394 nucleotide product of the wild-type allele.

All mice were uninephrectomized under general anesthesia five days before the BSA injections began. The first group of animals received daily injections of BSA (Sigma A-7906; Sigma Chemical Company, St. Louis, MO, USA) at a dose of 10 mg/g body weight until the animals were killed. The BSA was dissolved in saline (0.33 mg/mL) and injected into the peritoneal cavity, a dose that we used previously in the rat model of BSA-induced overload proteinuria [6]. A small number of animals in the first pilot study developed pulmonary edema. Two modifications in the BSA injection protocol prevented this complication and were implemented in all subsequent studies. First, the BSA preparation was changed to low endotoxin BSA (Sigma A-9430). Second, the intraperitoneal injections were given five rather than seven days each week until the animals were killed. The final dose of 10 mg BSA/g body weight was reached by incremental increases in the dose over the first week, beginning with 2 mg/g body weight. All control animals received intraperitoneal injections of an equal volume of saline on an identical schedule.

For the first pilot study, groups of mice were sacrificed on day 10 ($N = 8$ BSA-injected and 4 saline-injected controls) and day 24 ($N = 4$ BSA-injected and 4 saline-injected controls). Between days 8 and 10, individual mice were placed in metabolic cages, and all urine that was spontaneously voided over a 48-hour period was collected for determination of urinary protein:creatinine ratios. Animals were killed by exsanguination under general anesthesia. Pieces of the renal cortex were snap frozen in 2-methylbutane that was precooled in liquid nitrogen, and the tissue was stored at −80°C for subsequent immunofluorescence staining. Small cortical pieces were also fixed in 4% paraformaldehyde/1% gluteraldehyde dissolved in 0.1 mol/L phosphate-buffered saline and were processed for electron microscopy.

Renal gene expression time course study in *Timp-1*–deficient and wild-type mice

Male *Timp-1*–deficient and wild-type mice were allowed to reach 20 g body weight before the study began. BSA-overload proteinuria was induced in six *Timp-1*–deficient and six wild-type uninephrectomized male mice using the protocol that was developed and described previously in this article. Two animals from each group were sacrificed at one, two, and six weeks, respectively. These time points were selected to evaluate early renal events because of our concern that significant changes in gene expression patterns may not be sustained during the course of the disease, and at a late time point when we expected significant interstitial fibrosis to be present histologically (week 6). One saline-injected control from each group was sacrificed at each time point (except the 6-week mutant TIMP group). This sample size was chosen for the pilot study in order that samples of renal RNA from each individual animal (total = 17) could be loaded into a single gel for comparison of the temporal pattern of gene expression. All animals were sacrificed by exsanguination under general anesthesia. The single kidney was frozen in liquid nitrogen and stored at −80°C for subsequent RNA extraction.

Severity of interstitial fibrosis in *Timp-1* wild-type and deficient mice with overload proteinuria

Male *Timp-1*–deficient and wild-type mice began the study weighing an average of 20 g. At the termination of the study, the average weight of both groups of mice was 22 g. Prior to the initiation of this study, we determined that interstitial fibrosis developed in mice with two kidneys, and the uninephrectomy step was eliminated in this final protocol. [In the pilot study, the mean total kidney collagen content in wild-type mice was 0.42 mg (saline injected), 0.75 mg (single kidney BSA-injected), and 0.67 mg (two kidney BSA-injected)]. The availability of two kidneys made it possible to perform immunostaining and total kidney collagen assays in all animals. Four groups of animals were studied: BSA-overload proteinuria ($N = 8$) and saline controls ($N = 4$) in wild-type mice and BSA-overload proteinuria ($N = 8$) and saline controls ($N = 4$) in *Timp-1*–deficient mice. Each animal received an intraperitoneal injection of BSA in saline or saline alone five days each week for a total of six weeks. Prior to sacrifice, each individual animal was placed in a metabolic cage for 48 hours to collect spontaneously voided urine. All animals were killed after six weeks of injections by exsanguination under general anesthesia. Both kidneys were snap frozen and stored at −80°C. The total collagen content of the left kidney was determined. Immunohistochemical studies were performed on the right kidney.

Measurement of renal gelatinase activity

Groups of six male wild-type and six male *Timp-1*–deficient mice were given seven daily injections of BSA. These mice were not uninephrectomized. Urinary protein excretion rates were measured on day 6. All animals were killed on day 8, and the kidneys were harvested to measure total renal gelatinase activity by gel zymography.

All animal experimentation described was conducted according to the guidelines established by the Canadian Council on Animal Care and the National Research Council. All animals were fed standard mouse chow and were given water ad libitum.

Biochemical studies

Total urinary protein was measured in the 48-hour urine collections using the Bio-Rad protein assay (Bio-Rad Laboratories Canada Ltd., Mississauga, Ontario, Canada). Results were expressed as mg protein per μmol or mg urinary creatinine. Plasma and urinary creatinine levels were measured using the Kodak Ektachem Clinical Chemistry slide technique in the Hospital for Sick Children Clinical Biochemistry Department. Urinary BSA levels were measured by radial immounodiffusion using a rabbit antibovine albumin antibody (Cappel Division, Organon Tehnika Corp., West Chester, PA, USA).

The total kidney collagen was calculated as previously described [6] based on measurements of the hydroxyproline concentration in kidney homogenates, according to the technique of Kivirikko, Laitinen, and Prockop [23]. Collagen was assumed to contain 12.7% hydroxyproline by weight. The final results, based on the wet weight of the kidney, were expressed as milligrams of collagen per kidney.

Renal immunofluorescence studies

The accumulation of interstitial matrix proteins in the renal interstitium was assessed semiquantitatively using a slight modification of our previously described method [5]. In brief, random cortical interstitial fields contained within a 10 × 10 mm eyepiece grid (magnification ×300) were each assigned an arbitrary staining score of normal or increased based on the area of positive staining. All equivocal scoring patterns were assigned a normal score. The investigator (A.A.E.) was blinded to the animal group at the time of the analysis. The results were expressed as the percentage interstitial fields with a definite increase in interstitial staining. The primary antibodies used were sheep antihuman collagen I, goat antihuman collagen III (Southern Biotechnology Associates, Birmingham, AL, USA), and goat antihuman fibronectin (Dimension Laboratories, Inc., Mississauga, Ontario, Canada). Selected tissue sections were also stained with a murine monoclonal antibody to bovine dental pulp

TIMP-1 (Oncogene Research Products, Cambridge, MA, USA) or rabbit antihuman TIMP-2 (Chemicon International Inc., Temecula, CA, USA). The secondary antisera were fluorescein isothiocyanate (FITC)-conjugated rabbit anti-sheep IgG, FITC-conjugated rabbit antigoat IgG (Organon Technika Corp.), and FITC-conjugated goat anti-mouse IgG (Zymed Laboratories, San Francisco, CA, USA). All FITC-conjugated antisera were preabsorbed with normal mouse plasma and were shown to be nonreactive with control kidney sections.

For the initial study when the murine protein-overload model was being developed and characterized, additional immunohistochemical studies were performed. The numbers of interstitial macrophages were counted after staining with a rat monoclonal antibody directed against the mouse Mac-1 antigen (Sera-Lab Division, Dimension Laboratories, Inc., Mississauga, Ontario, Canada) using the dual fluorchrome labeling and enumeration technique that we have described elsewhere [24]. FITC-conjugated antibodies used were rabbit antirat lgG $F(ab')_2$ (Cappel Division, Organon Technika Corp.) and goat antirabbit lgG $F(ab')_2$ (Zymed Laboratories Inc.). The degree of glomerulosclerosis was determined by calculating the percentage of glomeruli (from an average of 50 glomeruli evaluated per animal) that showed increased staining for collagen I, collagen III, and fibronectin. The patterns of deposition of BSA, the murine third component of complement (C3) and mouse immunoglobulins were evaluated after staining cryosections with FITC-conjugated rabbit anti-bovine albumin, FITC-conjugated goat anti-mouse C3, or FITC-conjugated goat-anti-mouse immunoglobulins IgA + IgG + IgM (Cappel Division, Organon Technika Corp.).

Ultrastructural studies

Pieces of renal cortex from the animals in the first study were processed for electron microscopy. Following paraformaldehyde/gluteraldehyde fixation, the tissues were postfixed in 1% osmium tetroxide, dehydrated in graded acetone, and embedded in an Epon-Araldite mixture. Sections were cut at 50 nm, stained with uranyl acetate and lead citrate, and examined with a Philips 400 electron microscope.

Northern blot analysis

Total kidney RNA was isolated according to the guanidinium-isothiocyanate cesium chloride method of Chirgwin et al, and Northern blotting was performed according to standard methods [25]. We obtained autoradiographs and quantitated the bands by laser densitometry. The density reading of each band on the autoradiograph was adjusted for any RNA loading inequality, as we have previously described, based on the density reading of the closest ethidium bromide-stained ribosomal band [5]. The results were expressed in arbitrary densitometric units standardized to a mean value of 1.0 unit for the control group.

Table 1. Urinary protein levels on day 10

	BSA overload	Controls
Urinary total protein (mg/μmol creatinine) $\times 10^{-3}$	87 ± 30[a]	10 ± 1
Urinary BSA levels (mg/μmol creatinine) $\times 10^{-3}$	1.3 ± 0.6[a]	0 ± 0

Results are mean ± 1 SD.
[a] $P < 0.05$ compared with saline-injected controls

The cDNA probes used were murine TIMP-1 [26] and murine TIMP-3 [27] (supplied by Dr. R. Khokha, Ontario Cancer Institute, University of Toronto, Toronto, Ontario, Canada), murine TIMP-2 [28] and TIMP-4 [29] (supplied by Dr. Kevin Leco, Department of Medical Biochemistry, University of Calgary, Alta, Canada), rat TGF-β1 (supplied by Dr. S.W. Qian, National Cancer Institute, Bethesda, MD, USA) [30], rat α1(I) procollagen (supplied by Dr. S. Thorgeirsson, National Cancer Institute, Bethesda, MD, USA) [31], murine α1(III) procollagen (supplied by Dr. B. deCrombrugghe, Anderson Cancer Center, The University of Texas, Houston, TX, USA) [32], and murine α2(IV) procollagen (supplied by Dr. M. Kurkinen, Rutgers Medical School, University of New Jersey, Piscataway, NJ, USA) [33].

Gelatin zymography

Gelatin zymography was performed according to the method reported by Kenagy et al [34]. In brief, a piece of renal cortex was snap frozen in liquid nitrogen and stored at −70°C prior to analysis. The frozen kidney pieces were individually ground into a fine powder using a mortar and pestle that had been prechilled with dry ice. The samples were extracted with 0.05 mol/L Tris buffer, pH 7.5, containing 0.01 mol/L $CaCl_2$, 2.0 mol/L guanidine, and 0.2% Triton-X 100, and dialyzed against 0.05 mol/L Tris, pH 7.5, 0.2% Triton-X 100 for 48 hours at 4°C. The samples were centrifuged for five minutes (14,000 × *g*). The supernatant was removed, and the protein concentration was determined using the Biorad protein assay. The protein extracts (10 μg/kidney sample) were loaded into individual wells of a 10% sodium dodecyl sulfate-polyacrylamide gel (SDS-PAGE) containing 1 mg/mL porcine skin gelatin (Sigma Chemical Company) as the substrate. The outer wells of each gel were loaded with human MMP-2 and MMP-9 standards (Chemicon International Inc.). Electrophoresis was performed under nonreducing conditions. The gel was rinsed with 2.5% Triton X-100 at room temperature for 30 minutes to removed the SDS. After incubation for 17 to 20 hours at 37°C in a solution containing 50 mmol/L Tris, pH 7.8, and 10 mmol/L $CaCl_2$, the gel was stained with Coomassie blue (0.002%). The stained gel was pho-

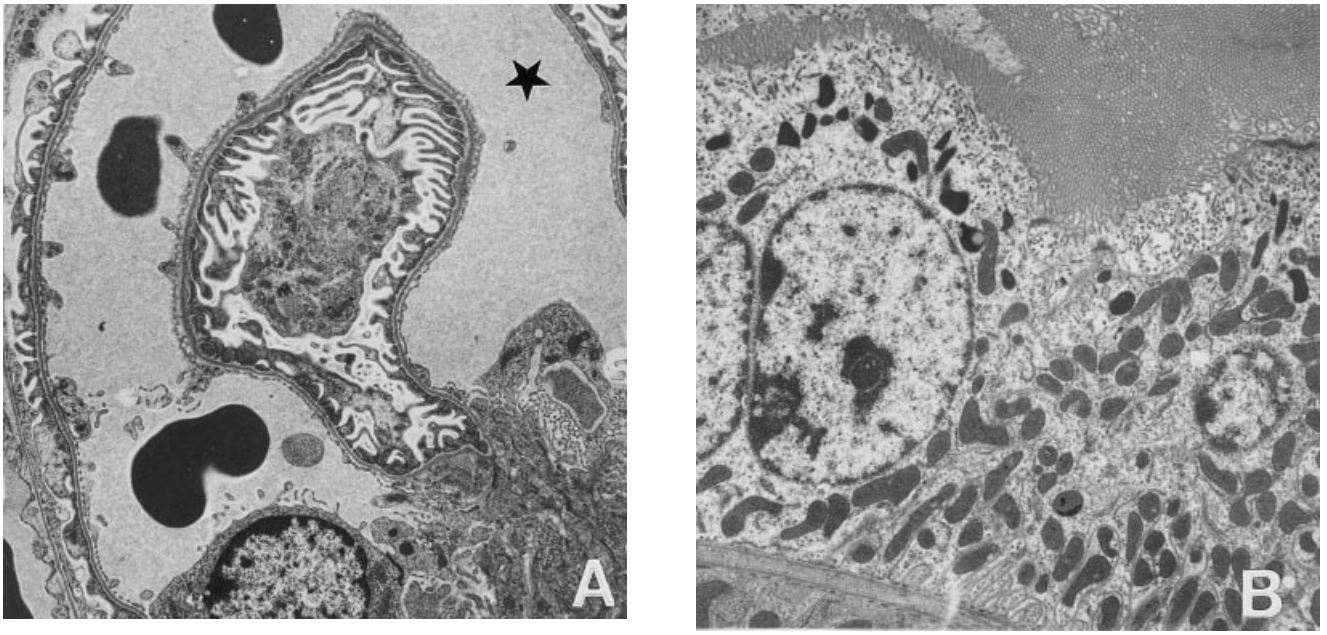

Fig. 1. Electron photomicrographs of a mouse kidney after 10 days of overload proteinuria. (*A*) Proteinaceous material is deposited within the endothelial space of some capillary loops (star). At a higher magnification (data not shown), many prominent vacuoles are seen in glomerular epithelial cells. (*B*) Proximal tubular cells appear normal. No electron dense deposits were observed. Numerous microvilli in cross-section are appreciated in the upper region of the photomicrograph. Similar findings were noted on day 24 (magnification ×4900).

tographed, and the density of the lytic bands was quantitated using the NIH image analysis program.

Statistical analysis

Statistical analyses were performed with the Mann Whitney *U*-test. Probability values < 0.05 were considered significant.

RESULTS

Characterization of murine protein-overload proteinuria model

To produce a murine model of proteinuria and kidney fibrosis, the model of protein-overload proteinuria previously developed in rats was adapted for mice. Repeated intraperitoneal injections of BSA (10 mg/g body weight), given five days weekly until the mice were sacrificed at six weeks, caused significant renal pathologic changes. The mice developed significant proteinuria, a component of which was the injected BSA (Table 1). Ultrastructural examination of the proteinuric kidneys corroborated the finding of immunofluorescence microscopy with no evidence of electron dense deposits within the kidney to suggest renal immune complex deposition (Fig. 1). Immunofluorescence staining showed large glomerular deposits resembling protein reabsorption droplets that stained for BSA, C3, and immunoglobulins. The tubular and glomerular basement membranes showed faint linear staining for BSA in the proteinuric but not control animals. Occasional tubular protein reabsorption droplets were seen, particularly after staining for C3 or immunoglobulins. The tubulointerstitial disease was characterized by an interstitial infiltrate of macrophages (Fig. 2). A few interstitial cells also expressed surface immunoglobulins. The proteinuric animals developed renal fibrosis, as evidenced by the accumulation of matrix proteins in the interstitium (Fig. 3) and glomerulosclerosis (Fig. 4). These pathologic changes are similar to the findings in rats with BSA-induced overload proteinuria [6].

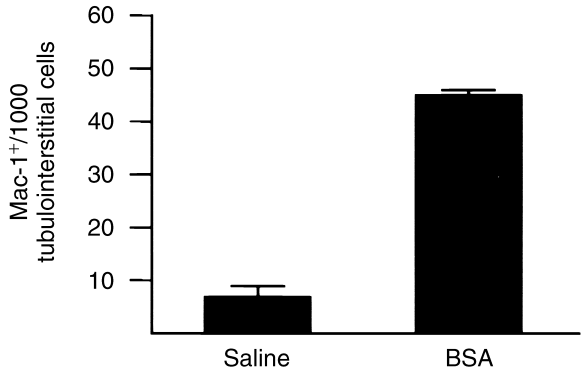

Fig. 2. Interstitial inflammation in mice with overload proteinuria. The graph illustrates the mean number of Mac-1$^+$ renal interstitial macrophages after 10 days of intraperitoneal injections of saline or BSA (N = 2 mice per group).

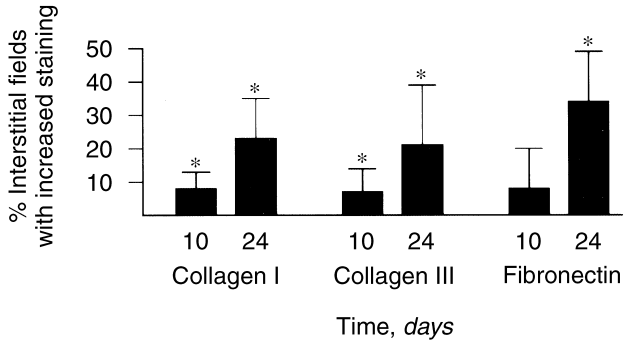

Fig. 3. Interstitial fibrosis in mice with overload proteinuria. The graph illustrates the average number of interstitial fields with increased staining for collagen I, collagen III, and fibronectin after 10 ($N = 8$) and 24 ($N = 4$) days of BSA injections. This assessment was performed by assigning a value of 0 to the percentage of fields with increased interstitial staining in the saline-injected controls ($N = 7$). *$P < 0.05$ compared with saline-injected control mice.

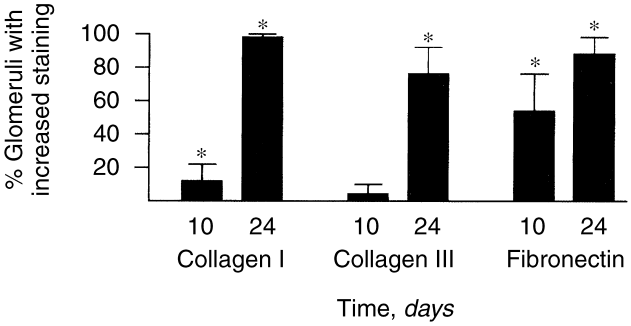

Fig. 4. Glomerulosclerosis in mice with overload proteinuria. The graph illustrates the average number of glomerular cross sections with increased staining for collagen I, collagen III, and fibronectin after 10 ($N = 8$) and 24 ($N = 4$) days of BSA injections. This assessment was performed by assigning a value of 0 to the percentage of glomerular cross sections with increased staining in the saline-injected controls ($N = 7$). *$P < 0.05$ compared to saline-injected control mice.

Renal gene expression time course study

Renal *Timp-1* mRNA levels were increased in the wild-type mice with overload proteinuria, ranging from four- to tenfold relative to control levels (Fig. 5). The constitutive *Timp-2* gene is abundantly expressed in normal mouse kidneys (wild-type and *Timp-1* deficient), and the levels changed little from control values during the course of BSA-induced overload proteinuria (Fig. 6). *Timp-3* gene transcripts are also abundant in normal mouse kidneys. In proteinuric mice, renal *Timp-3* mRNA levels were twice control levels on day 7, but were similar to control levels on days 14 and 42 (Fig. 7). *Timp-4* mRNA transcripts were not detected by Northern blotting in any of the renal RNA samples (not shown). A positive band was identified when the *Timp-4* probe was hybridized with murine heart RNA, verifying that appropriate hybridization conditions had been used. The pat-

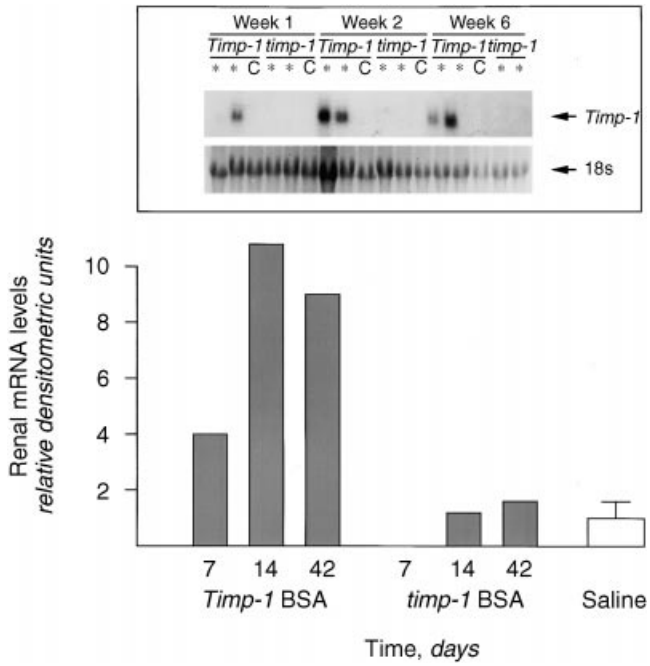

Fig. 5. Time-course study of renal *Timp-1* mRNA (0.9 kb) steady-state levels in mice with overload proteinuria. The autoradiograph of the Northern blot is shown above where the asterisk indicates BSA-injected mice and C indicates saline-injected controls. The graph summarizes the densitometric results (mean of 2 animals) expressed in arbitrary units where 1.0 unit is the mean densitometric value obtained from the five saline-injected controls. *Timp-1* indicates wild-type mice, and *timp-1* indicates deficient mice.

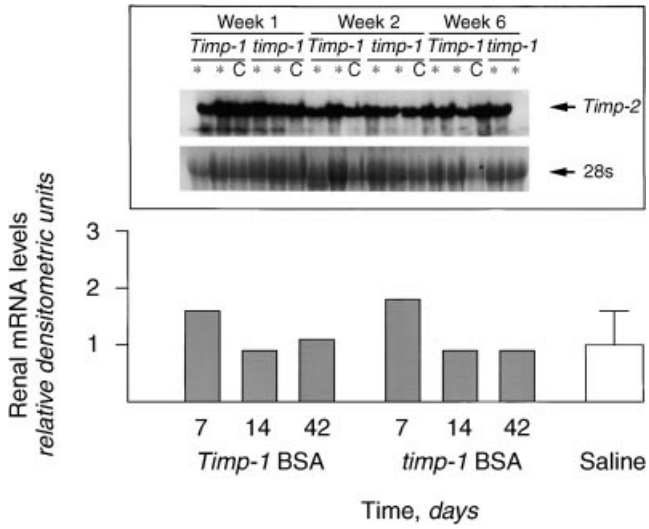

Fig. 6. Time-course study of renal *Timp-2* steady-state mRNA (3.5 kb) levels in mice with overload proteinuria. The autoradiograph of the Northern blot is shown above where the asterisk indicates BSA-injected mice and C indicates saline-injected controls. The graph summarizes the densitometric results (mean of 2 animals) expressed in arbitrary units where 1.0 unit is the mean densitometric value obtained from the five saline-injected controls. A weaker second band visualized at 1.0 kb showed a similar expression profile (data not shown). *Timp-1* indicates wild-type mice, and *timp-1* indicates deficient mice.

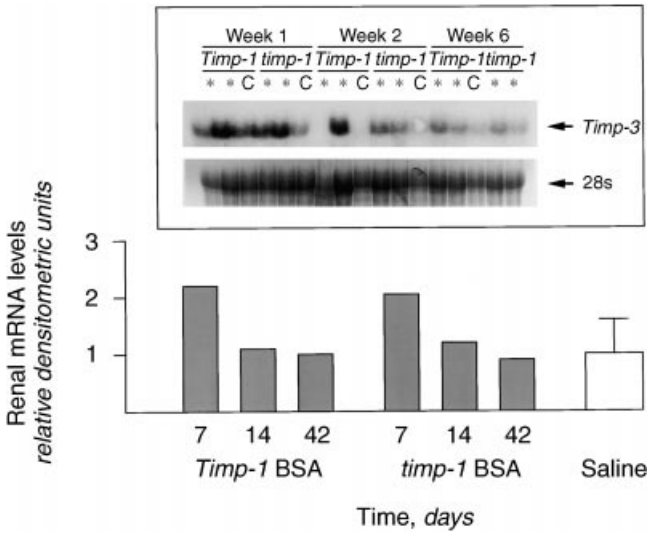

Fig. 7. Time-course study of renal *Timp-3* steady-state mRNA (4.5 kb) levels in mice with overload proteinuria. The autoradiograph of the Northern blot is shown above where the asterisk indicates BSA-injected mice and C indicates saline-injected controls. The graph summarizes the densitometric results (mean of 2 animals) expressed in arbitrary units where 1.0 unit is the mean densitometric value obtained from the five saline-injected controls. *Timp-1* indicates wild-type mice, and *timp-1* indicates deficient mice.

Table 2. Murine protein-overload kidney mRNA levels

	Timp-1 BSA overload ($N = 2$)	*timp-1* BSA overload ($N = 2$)	Saline controls ($N = 5$)
Procollagen α1(I)			
Week 1	1.6 ± 0.8	2.5 ± 0.4	
Week 2	3.2 ± 0.1	1.7 ± 0.8	1.0 ± 0.1
Week 6	2.6 ± 0.3	2.1 ± 0.1	
Procollagen α1(III)			
Week 1	3.0 ± 1.8	3.2 ± 2.1	
Week 2	2.3 ± 0.6	1.9 ± 0.6	1.0 ± 0.5
Week 6	1.8 ± 0.1	1.5 ± 0.6	
Procollagen α2(IV)			
Week 1	1.8 ± 1.2	1.8 ± 0.5	
Week 2	0.7 ± 0.4	1.0 ± 0.4	1.0 ± 0.4
Week 6	1.2 ± 0.2	1.2 ± 0.2	
TGF-β1			
Week 1	1.8 ± 0.6	1.3 ± 0.2	
Week 2	1.4 ± 0.4	1.0 ± 0.2	1.0 ± 0.3
Week 6	1.1 ± 0.1	1.5 ± 0.3	

Results are densitometric results in arbitrary units presented as mean for protein-overload; mean ± 1 SD for saline controls. *Timp-1* refers to wild-type mice, and *timp-1* refers to mutant mice.

terns of expression of genes encoding α1(I), α1(III), and α2(IV) procollagens and TGF-β1 are summarized in Table 2. Apart from *Timp-1*, the pattern of renal gene expression was very similar in both wild-type and *Timp-1*–deficient mice with overload proteinuria. TIMP-1 and TIMP-2 protein could not be identified in frozen kidney sections by immunofluorescence microscopy using the primary antibodies used in this study.

Severity of interstitial fibrosis in Timp-1 wild-type and deficient mice with overload proteinuria

After six weeks of BSA-induced overload proteinuria, the severity of the renal interstitial fibrosis was similar in the wild-type and *Timp-1*–deficient mice. Both BSA-treated groups had similar degrees of significant proteinuria compared with the saline-injected animals (Table 3). The severity of the interstitial fibrosis was similar in both proteinuric groups based on the increase in kidney weight (Table 3), total kidney collagen content (Fig. 8), and percentage of interstitial fields with an increased area of staining for fibronectin (Figs. 9 and 10).

Renal gelatinase activity in mice with overload proteinuria

The day prior to sacrifice (that is, day 7), the two experimental groups used for the zymographic studies were confirmed to have significant proteinuria that was similar in quantity in both experimental groups: 0.7 ± 0.6 mg/mg creatinine and 0.6 ± 0.7 mg/mg creatinine for the wild-type and *Timp-1*–deficient mice, respectively. Values for control mice in our laboratory were consistently less than 0.1 mg/mg creatinine. In preparation for gelatin zymography, we first determined that the quantity of protein loaded into each well (10 μg) was in the linear range of the assay. Shown in Figure 11, protein concentrations between 2 and 32 μg were found to produce linear results ($r = 0.98$ to 0.99). After seven days of overload proteinuria, the mean renal MMP-9 (gelatinase B) activity was slightly increased in the *Timp-1*–deficient animals, but this difference was not statistically significant (Fig. 12). The mean MMP-9 activity expressed in arbitrary densitometric units was 1.0 ± 0.1 compared with 1.3 ± 0.2 units for the wild-type and *Timp-1*–deficient proteinuric groups, respectively ($P = 0.053$). In comparison to MMP-9 activity, MMP-2 activity was weak and similar in all kidneys.

DISCUSSION

The murine model of BSA-induced overload proteinuria is an experimental model of renal disease characterized by mild glomerulosclerosis, interstitial inflammation, and interstitial fibrosis. These histologic features and the absence of renal immune deposits suggest that the pathogenesis of the renal injury is similar to that of the rat model of protein-overload proteinuria, with proteinuria itself contributing to tubulointerstitial damage [6, 35]. Changes in the pattern of renal gene expression initially suggested that both increased rates of matrix protein synthesis and TIMP-1–mediated inhibition of matrix remodeling by metalloproteinases could contribute to the genesis of renal interstitial scarring.

Our finding that the severity of interstitial fibrosis was

Table 3. Overload proteinuria in *Timp-1* and *timp-1* mice: Results at six weeks

	Timp-1 mice		*timp-1* mice	
	BSA overload ($N = 8$)	Saline controls ($N = 4$)	BSA overload ($N = 8$)	Saline controls ($N = 4$)
Urinary protein (μg/μmol creatinine)	16.3 ± 19.7[a]	0.3 ± 0.1	16.2 ± 7.8[b]	0.3 ± 0.1
Plasma creatinine (μmol/L)	32 ± 19	22 ± 7	27 ± 5[b]	21 ± 1
Final kidney weight (mg)	211 ± 25[a]	167 ± 14	214 ± 4[b]	149 ± 11

Timp-1 refers to wild-type mice, and *timp-1* refers to mutant mice.
[a] $P < 0.05$ BSA compared with saline-injected wild-type mice
[b] $P < 0.05$ BSA compared with saline-injected *Timp-1*–deficient mice

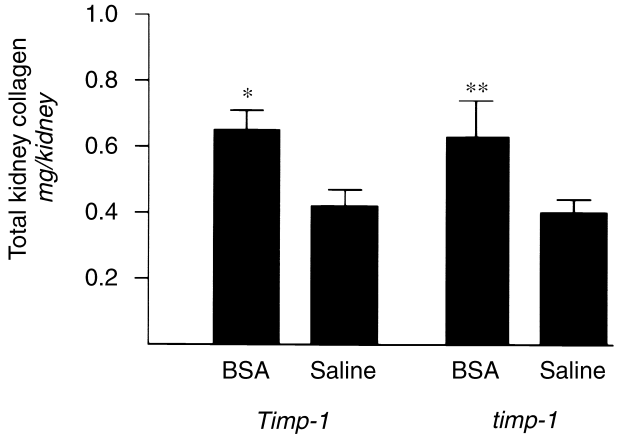

Fig. 8. Mean total kidney collagen content. After six weeks of BSA injections, the total kidney collagen content is significantly increased compared with saline-injected controls. The increase in the kidney collagen content is similar in wild-type mice (*Timp-1*) and deficient mice (*timp-1*). *$P < 0.05$ BSA compared with saline-injected wild-type mice; **$P < 0.05$ BSA compared with saline-injected deficient *timp-1* mice.

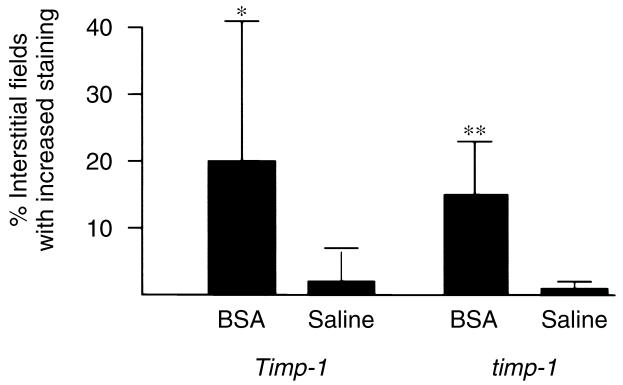

Fig. 9. Interstitial fibrosis after six weeks of overload proteinuria. The graph illustrates the mean number of interstitial fields with increased staining for fibronectin in wild-type mice (*Timp-1*) and deficient mice (*timp-1*). *$P < 0.05$ BSA compared with saline-injected wild-type mice; **$P < 0.05$ BSA compared with saline-injected deficient *timp-1* mice.

not altered by genetic deficiency of TIMP-1 was somewhat surprising based on evidence from numerous studies that increased renal TIMP-1 production characterizes most progressive renal diseases [36]. One likely explanation is that renal expression of *Timp-1* is genetically redundant in mice. In the present study, renal mRNA levels for *Timp-2* and *Timp-3* were constitutively high, and they may have compensated for the deficiency in *Timp-1.* Other metalloproteinase inhibitors, both known (such as α2-macroglobulin) and unknown, may also play a compensatory role. Indeed, our failure to document a significant difference in renal gelatinase activity between proteinuric mice in the presence and absence of TIMP-1 supports the existence of a compensatory response in the face of *Timp-1* deficiency. Future studies in mice genetically deficient in two or more metalloproteinase inhibitors should be able to test this hypothesis.

TIMP-1 is an efficient inhibitor of MMP-9 (gelatinase B) because of its ability to bind to both the proenzme as well as its active form. The results of our zymographic studies of renal MMP-9 activity after seven days of proteinuria showed increased activity in the TIMP-1–deficient group, but this difference was not statistically significant. We cannot rule out the possibility that a significant difference in net renal metalloproteinase activity was present at other critical time points, but it is noteworthy that *Timp-1* mRNA levels were already increased fourfold above control levels at the time that MMP-9 activity was measured. We have recently found similar results of renal MMP-9 activity in a murine model of unilateral ureteral obstruction with increased activity in the TIMP-1–deficient mice, to a degree that is borderline significant. In that study, the severity of interstitial fibrosis was also not attenuated by TIMP-1 deficiency (Kim et al, manuscript in preparation). In addition to the gelatinases, members of the stromelysin and interstitial collagenase families of metalloproteinase may also be inhibited by TIMP-1, and these proteases are also likely to contribute to matrix remodeling during interstitial fibrogenesis. However, we were unable to detect sufficient casein-degrading activity in the kidney homogenates to make meaningful comparisons between the two experimental groups (data not shown). It is worth comment that these zymography results, which reflect total renal MMP-9 activity, do not exclude that possibility of biologically significant regional variation in MMP-9 activity within selected compartments within the kidney.

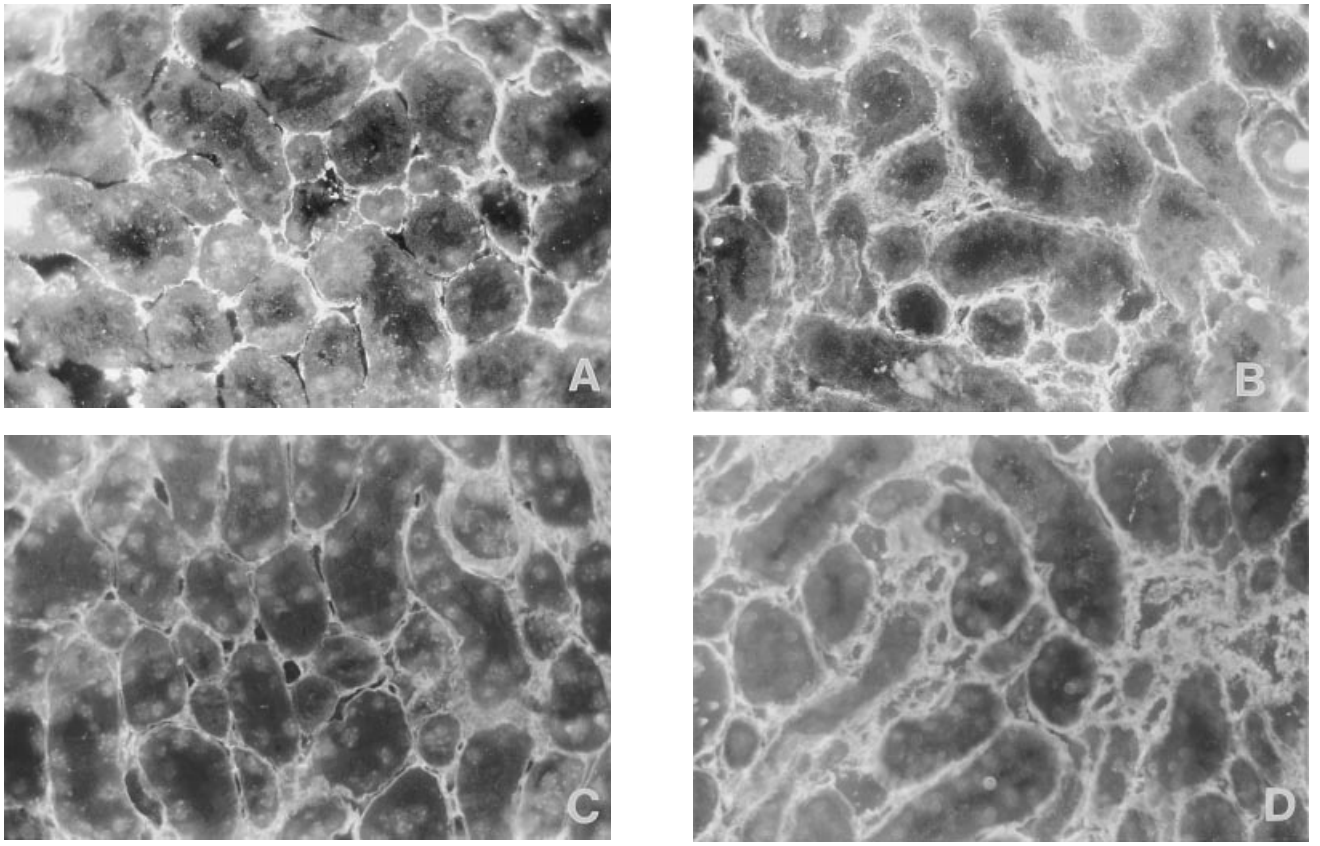

Fig. 10. Immunofluorescence photomicrographs illustrating renal interstitial fibrosis in mice with overload proteinuria for six weeks. (*A*) Collagen III staining in a control wild-type mouse and (*B*) collagen III staining in a proteinuric wild-type mouse. A similar pattern was observed in the *Timp-1* deficient mice. (*C*) Fibronectin staining in a control *Timp-1* deficient mouse and (*D*) fibronectin staining in a proteinuric *Timp-1* deficient mouse. A similar pattern was found in the wild-type mice (magnification ×240).

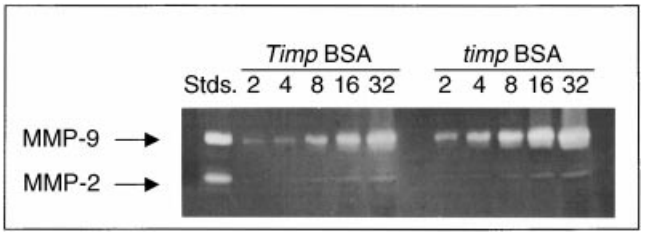

Fig. 11. Gelatin zymography illustrating MMP-9 and MMP-2 activity in homogenates of renal tissue after seven days of overload proteinuria. Lane 1, MMP standards; lanes 2 through 6 were loaded with increasing concentrations of kidney homogenates (2 to 32 μg protein) from a *Timp-1* mouse; lanes 7 through 11 were loaded with increasing concentrations (2 to 32 μg protein) from a *timp-1* mouse. The results show that the gelatinase activity is linearly related to the protein concentration in this range ($r = 0.99$).

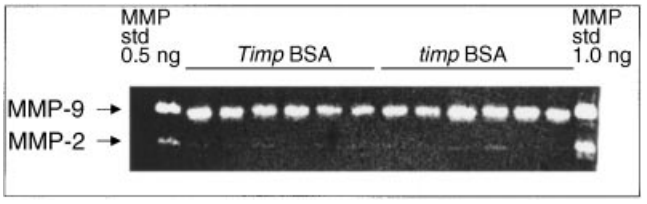

Fig. 12. Gelatin zymography illustrating MMP-9 and MMP-2 activity in kidney homogenates prepared from wild-type mice (*Timp-1*) and deficient mice (*timp-1*) after seven days of BSA-induced overload proteinuria. Each lane represents a sample (10 μg protein) from individual mice.

We can only speculate on the cellular origin of the TIMP-1 protein in the murine protein-overload model, as we have been unable to localize it by immunostaining using the antibodies that are currently available. However, this murine model appears very reminiscent of the rat model that has been induced using a similar experimental protocol. In the rat model, TIMP-1 protein was found in the interstitial space, suggesting that is had been secreted by adjacent cells [6]. In situ hybridization studies in the rat model identified transcripts in both tubular and interstitial cells [17].

Traditional thinking suggests that decreased renal metalloproteinase activity should worsen fibrosis because of reduced rates of degradation of matrix proteins. In support of this viewpoint, Sebekova et al found that

treatment with a protease cocktail (phlogenzyme) for six to seven weeks decreased renal fibrosis in the rat remnant kidney model and the Goldblatt-hypertension model [37, 38]. However, fibrogenesis, particularly at some extrarenal sites, has been associated with a net increase in metalloproteinase activity. For example, in a study of cardiac fibrosis in humans with idiopathic dilated cardiomyopathy, Gunja-Smith et al found a 30-fold increase in the net collagenase and gelatinase activity associated with a significant increase in total collagen [39]. They also noted a decrease in the formation of mature pyridinoline cross-links, the major mature collagen cross-link in the heart. These investigators suggested that an increase in cardiac metalloproteinase activity in the face of increased collagen synthesis is harmful because of the ability of metalloproteinases to degrade collagen fibrils into poorly cross-linked, immature, and unstable fibrils. The final predicted outcome would then be a vicious cycle of collagen synthesis and destruction with misdirected deposition of unstable collagen [40]. Thus, depending on the specific sequence of fibrogenic events, metalloproteinase activity may have protective or damaging consequences.

Metalloproteinases and their inhibitors have other activities beyond their role in matrix remodeling. For example, there is increasing evidence that members of the metalloproteinase family may have proinflammatory effects. Using anti-metalloproteinase-2 (MMP-2) ribozymes, Turck et al reported significant changes in cultured glomerular mesangial cells [41]. When MMP-2 production was inhibited, the mesangial cells reverted from an "active" phenotype of proliferation and matrix synthesis to a "quiescent" phenotype. Rat mesangial cells transfected with a cDNA encoding the rat stromelysin homologue, transin, responded with an increased rate of proliferation [42]. In vivo inhibition of metalloproteinase activity using the MMP inhibitor BB-1101 has recently been reported to decrease glomerular hypercellularity and glomerular matrix accumulation in rats with anti-Thy-1 nephritis [43]. Other reported biologic effects include growth-promoting activity and inhibition of angiogenesis. Based on this body of evidence, it is possible that the severity of the acute renal injury in the *Timp-1*–deficient mice with BSA-induced overload proteinuria was actually more severe, but that the subsequent fibrogenic response was attenuated by the lack of TIMP-1. Against this possibility, we found that the tubular cell mitotic index and the number of vimentin-positive regenerating tubules were similar in both proteinuric groups after seven days of BSA injections (data not shown).

The results of the present study raise a potentially important question. That is, if in fact renal induction of the *Timp-1* gene does not have a significant effect on renal metalloproteinase activity and the ensuing fibrogenic response, what is its role? As reviewed in the introduction, most progressive renal diseases are characterized by increased *Timp-1* expression. This response is not unique to the kidney but also characterizes fibrosis in other organs such as the liver [44]. Indeed, TIMP-1 is already known to have many other effects that are not dependent on its ability to inhibit metalloproteinases. Some of these effects include growth factor activity, inhibition of apoptosis, inhibition of angiogenesis, changes in cell morphology, and stimulation of gonadal steroidogenesis [45, 46]. Further studies are indicated to explore a role for TIMP-1 in renal disease that is independent of its MMP-inhibitory activities.

In summary, the experimental model of BSA-induced overload proteinuria in mice should be a useful model for investigating the molecular basis of renal fibrosis in genetically engineered mice. Genetic deficiency of TIMP-1 does not appear to affect the severity of interstitial fibrosis at six weeks in mice with protein-overload proteinuria. Whether these findings are unique to this renal disease model deserves further investigation. Our findings indicate that TIMP-1 deficiency results in a small but statistically insignificant increase in total renal MMP-9 activity, raising the possibility of genetic redundancy of *Timp-1*, possibly because of the high renal constitutive levels of *Timp-2* and/or *Timp-3*. Future studies need to consider the multifunctionality of TIMP-1 and the possibility that its induced expression in renal disease might modulate the renal response to injury via one of its metalloproteinase-independent effects.

ACKNOWLEDGMENTS

Sources of financial support for this work include grants from the Medical Research Council of Canada MT-11553 (A.A.E.), the Hospital for Sick Children Research Institute (A.A.E.), the Northwest Kidney Foundation (A.A.E.), the Leukemia Society of America (P.D.S.), National Institutes of Health grants DK54500 (A.A.E.), GM15325, and EY11279 (P.D.S.), and by Cancer Center Support grant P30 CA16056-21 at Roswell Park Cancer Institute. Part of this work was presented at the 31st annual meeting of the American Society of Nephrology and was published in abstract form (*J Am Soc Nephrol* 9:515A, 1998). The authors acknowledge the outstanding technical assistance of Ms. Lori McCulloch, Ms. Elaine Liu, and Ms. Diane Wing, and the assistance of Ms. Jennifer Samson and Ms. Jennifer Rieger with preparation of the manuscript.

Reprint requests to Dr. Allison Eddy, Division of Nephrology, Children's Hospital and Regional Medical Center, Mail Stop CH-46, 4800 Sand Point Way NE, Seattle, Washington 98105, USA.
E-mail: aeddy@u.washington.edu

REFERENCES

1. Eddy AA: Molecular insights into renal interstitial fibrosis. *J Am Soc Nephrol* 7:2495–2508, 1996
2. González-Avila G, Vadillo-Ortega F, Pérez-Tamayo R: Experimental diffuse interstitial renal fibrosis: A biochemical approach. *Lab Invest* 59:245–252, 1988
3. Davies M, Martin J, Thomas GJ, Lovett DH: Proteinases and glomerular matrix turnover. *Kidney Int* 41:671–678, 1992
4. Norman JT, Lewis MP: Matrix metalloproteinases (MMPs) in renal fibrosis. *Kidney Int* 49:S61–S63, 1996
5. Jones CL, Buch S, Post M, McCulloch L, Liu E, Eddy AA: The

pathogenesis of interstitial fibrosis in chronic purine aminonucleoside nephrosis. *Kidney Int* 40:1020–1031, 1991
6. Eddy AA, Giachelli CM: Renal expression of genes that promote interstitial inflammation and fibrosis in rats with protein-overload proteinuria. *Kidney Int* 47:1546–1557, 1995
7. Tang WW, Feng L, Xia Y, Wilson CB: Extracellular matrix accumulation in immune-mediated tubulointerstitial injury. *Kidney Int* 45:1077–1084, 1994
8. Duymelinck C, Deng JT, Dauwe SE, De Broe ME, Verpooten GA: Inhibition of the matrix metalloproteinase system in a rat model of chronic cyclosporine nephropathy. *Kidney Int* 54:804–818, 1998
9. Wu K, Setty S, Mauer SM, Killen P, Nagase H, Michael AF, Tsilibary EC: Altered kidney matrix gene expression in early stages of experimental disease. *Acta Anat* 158:155–165, 1997
10. Eddy AA: Interstitial inflammation and fibrosis in rats with diet-induced hypercholesterolemia. *Kidney Int* 50:1139–1149, 1996
11. Nakamura T, Ebihara I, Osada S, Takahashi T, Yamamoto M, Tomino Y, Koide H: Gene expression of metalloproteinases and their inhibitor in renal tissue of New Zealand black/white F1 mice. *Clin Sci* 85:295–301, 1993
12. Ishidoya S, Morrisey J, McCracken R, Klahr S: Delayed treatment with enalapril halts tubulointerstitial fibrosis in rats with obstructive nephropathy. *Kidney Int* 49:1110–1119, 1996
13. Sharma AK, Mauer SM, Kim Y, Michael AF: Altered expression of matrix metalloproteinase-2, TIMP, and TIMP-2 in obstructive nephropathy. *J Lab Clin Med* 125:754–761, 1995
14. Engelmyer E, van Goor H, Edwards DR, Diamond JR: Differential mRNA expression of renal cortical tissue inhibitor of metalloproteinase-1, -2, and -3 in experimental hydronephrosis. *J Am Soc Nephrol* 5:1675–1683, 1995
15. Schaefer L, Han X, Gretz N, Häfner C, Meier K, Matzkies F, Schaefer RM: Tubular gelatinase A (MMP-2) and its tissue inhibitors in polycystic kidney disease in the Han:SPRD rat. *Kidney Int* 49:75–81, 1996
16. Jones CL, Buch S, Post M, McCulloch L, Liu E, Eddy AA: Renal extracellular matrix accumulation in acute puromycin aminonucleoside nephrosis in rats. *Am J Pathol* 141:1381–1396, 1992
17. Eddy AA: Expression of genes that promote renal interstitial fibrosis in rats with proteinuria. *Kidney Int* 49:S49–S54, 1996
18. Rudofsky UH, Dilwith RL, Tung KSK: Susceptibility differences of inbred mice to induction of autoimmune renal tubulointerstitial lesions. *Lab Invest* 43:463–470, 1980
19. Maxwell PH, Ferguson DJ, Nicholls LG, Johnson MH, Ratcliffe PJ: The interstitial response to renal injury: Fibroblast-like cells show phenotypic changes and have reduced potential for erythropoietin gene expression. *Kidney Int* 52:715–724, 1997
20. Chen A, Wei CH, Sheu LF, Ding SL, Lee WH: Induction of proteinuria by adriamycin or bovine serum albumin in the mouse. *Nephron* 69:293–300, 1995
21. Soloway PD, Alexander CM, Werb Z, Jaenisch R: Targeted mutagenesis of TIMP-1 reveals that lung tumor invasion is influenced by TIMP-1 genotype of the tumor but not by that of the host. *Oncogene* 13:2307–2314, 1996
22. Jackson IJ, Lecras TD, Docherty AJ: Assignment of the TIMP gene to the murine X-chromosome using an inter-species cross. *Nucleic Acids Res* 15:4357, 1987
23. Kivirikko KI, Laitinen O, Prockop DJ: Modifications of a specific assay for hydroxyproline in urine. *Anal Biochem* 19:249–255, 1967
24. Eddy AA, Michael AF: Acute tubulointerstitial nephritis associated with aminonucleoside nephrosis. *Kidney Int* 33:14–23, 1988
25. Chirgwin JM, Przybyla AE, MacDonald RJ, Rutter WJ: Isolation of biologically active ribonucleic acid from sources enriched in ribonuclease. *Biochemistry* 18:5294–5299, 1979
26. Khokha R, Denhardt DT: On the use of anti-sense RNA: Down-regulation of mRNA encoding a metalloproteinase inhibitor. *Anticancer Res* 7:653–660, 1987
27. Leco KJ, Khokha R, Pavloff N, Hawkes SP, Edwards DR: Tissue inhibitor of metalloproteinases-3 (TIMP-3) is an extracellular matrix-associated protein with a distinctive pattern of expression in mouse cells and tissues. *J Biol Chem* 269:9352–9360, 1994
28. Leco KJ, Hayden LJ, Sharma RR, Rocheleau H, Greenberg AH, Edwards DR: Differential regulation of TIMP-1 and TIMP-2 mRNA expression in normal and Ha-ras-transformed murine fibroblasts. *Gene* 117:209–217, 1992
29. Leco KJ, Suneel SA, Taniguchi GT, Hawkes SP, Khokha R, Schultz GA, Edwards DR: Murine tissue inhibitor of metalloproteinases-4 (*Timp*-4): cDNA isolation and expression in adult mouse tissues. *FEBS Lett* 401:213–217, 1997
30. Qian SW, Kondaiah P, Roberts AB, Sporn MB: cDNA cloning by PCR of rat transforming growth factor β-1. *Nucleic Acids Res* 18:3059, 1990
31. Nakatsukasa H, Nagy P, Evarts RP, Hsia C-C, Marsden E, Thorgeirsson SS: Cellular distribution of transforming growth factor-β1 and procollagen types I III, and IV transcripts in carbon tetrachloride-induced rat liver fibrosis. *J Clin Invest* 85:1833–1843, 1990
32. Toman PD, de Crombrugghe B: The mouse type-III procollagen-encoding gene: Genomic cloning and complete DNA sequence. *Gene* 147:161–168, 1994
33. Kurkinen M, Bernard MP, Barlow DP, Chow LT: Characterization of 64-, 123- and 182-base-pair exons in the mouse α-2 (IV) collagen gene. *Nature* 317:177–179, 1985
34. Kenagy RD, Nikkari ST, Welgus HG, Clowes AW: Heparin inhibits the induction of three matrix metalloproteinases (stromelysin, 92-kD gelatinase, and collagenase) in primate arterial smooth muscle cells. *J Clin Invest* 93:1987–1993, 1994
35. Eddy AA: Interstitial nephritis induced by heterologous protein-overload proteinuria. *Am J Pathol* 135:719–733, 1989
36. Jernigan SM, Eddy AA: Experimental insights into the mechanisms of tubulointerstitial scarring, in *Mechanisms and Clinical Management of Chronic Renal Failure*, edited by El Nahas M, Anderson S, Oxford, Oxford University Press, 2000, pp 104–145
37. Sebekova K, Paczek L, Dammrich J, Ling H, Spustova V, Gaciong Z, Heidland A: Effects of protease therapy in the remnant kidney model of progressive renal failure. *Miner Electrolyte Metab* 23:291–295, 1997
38. Sebekova K, Dammrich J, Fierlbeck W, Krivosikova Z, Paczek L, Heidland A: Effect of chronic therapy with proteolytic enzymes on hypertension-induced renal injury in the rat model of Goldblatt hypertension. *Am J Nephrol* 18:570–576, 1998
39. Gunja-Smith Z, Morales AR, Romanelli R, Woessner JF Jr: Remodeling of human myocardial collagen in idiopathic dilated cardiomyopathy. *Am J Pathol* 148:1639–1648, 1996
40. Stetler-Stevenson WG: Dynamics of matrix turnover during pathologic remodeling of the extracellular matrix. *Am J Pathol* 148:1345–1350, 1996
41. Turck J, Pollock AS, Lee LK, Marti HP, Lovett DH: Matrix metalloproteinase 2 (gelatinase A) regulates glomerular mesangial cell proliferation and differentiation. *J Biol Chem* 271:15074–15083, 1996
42. Kitamura M, Shirasawa T, Maruyama N: Gene transfer of metalloproteinase transin induces aberrant behavior of cultured mesangial cells. *Kidney Int* 45:1580–1586, 1994
43. Steinmann-Niggli K, Ziswiler R, Küng M, Marti H-P: Inhibition of matrix metalloproteinases attenuates anti-Thy 1.1 nephritis. *J Am Soc Nephrol* 9:397–407, 1998
44. Iredale JP, Benyon RC, Pickering J, McCullen M, Northrop M, Pawley S, Hovell C, Arthur MJP: Mechanisms of spontaneous resolution of rat liver fibrosis: Hepatic stellate cell apoptosis and reduced hepatic expression of metalloproteinase inhibitors. *J Clin Invest* 102:538–549, 1998
45. Gomez DE, Alonso DF, Yoshiji H, Thorgeirsson UP: Tissue inhibitors of metalloproteinases: Structure, regulation and biological functions. *Eur J Cell Biol* 74:111–122, 1997
46. Guedez L, Stetler-Stevenson WG, Wolff L, Wang J, Fukushima P, Mansoor A, Stetler-Stevenson M: In vitro suppression of programmed cell death of B cells by tissue inhibitor of metalloproteinases-1. *J Clin Invest* 102:2002–2010, 1998